SMALL RAYED CRATER EJECTA RETENTION AGE CALCULATED FROM CURRENT CRATER PRODUCTION RATES ON MARS. F. J. Calef III[1], R. R. Herrick[2], and V. L. Sharpton[2], [1]Jet Propulsion Laboratory, Caltech, Pasadena, CA 91109, fcalef@jpl.nasa.gov, [2]Geophysical Institute, University of Alasaka Fairbanks, Fairbanks, AK. rherrick@gi.alaska.edu, buck.sharpton@alaska.edu.

Introduction: Ejecta from impact craters, while extant, records erosive and depositional processes on their surfaces. Estimating ejecta retention age (E_{ret}), the time span when ejecta remains recognizable around a crater, can be applied to estimate the timescale that surface processes operate on, thereby obtaining a history of geologic activity. However, the abundance of sub-kilometer diameter (D) craters identifiable in high-resolution Mars imagery has led to questions of accuracy in absolute crater dating and hence ejecta retention ages (E_{ret}). This research calculates the maximum E_{ret} for small rayed impact craters (SRC) on Mars using estimates of the Martian impactor flux adjusted for meteorite ablation losses in the atmosphere. In addition, we utilize the diameter-distance relationship of secondary cratering to adjust crater counts in the vicinity of the large primary crater Zunil.

Estimating Ejecta Retention Age: To estimate E_{ret}, we determined the current cratering rate production function (CPF) and use a randomly sampled distribution of SRC over a known surface area [1]. The crater production rate is typically expressed within a defined range of crater diameters (bin) and by the number of craters (N) impacting a surface over a given time period (e.g. N km^{-2} a^{-1}). We calculate this CPF from the published data of [2] for SRC primaries, adjusted for both spatial randomness [3] and atmospheric filtering of impactors in a 6mb atmosphere for D <30 m craters [4].

Corrections for Atmospheric Filtering: There are four asteroidal impactor types related to source material in the asteroid belt between Mars and Jupiter [4]: carbonaceous chondrites (cc) (75%), stony (16%), irons (9%) or icy (i.e. cometary material). Icy components, however, have a negligible effect on the production rate of sub-kilometer D craters in a 6mb atmosphere [5]. From these parameters and the estimates of crater survival per diameter bin [5], we reconstitute the original population for a given bin by multiplying the counts, $N(D)_{src}$, times the mass fraction of meteorite (A_{type} after [5]), then divided by the fraction of meteorites from the total impacting population expected to impact (N_{type}) and create a crater count for that D bin, N(D):

$$N(D)_{cp} = (A_{cc}N(D)_{src})/N_{cc} + (A_{stony}N(D)_{stony})/N_{stony} + (A_{iron}N(D)_{iron})/N_{iron} \quad (1)$$

thereby estimating the crater population that would have occurred in the absence of an atmosphere. This correction nearly doubles the crater counts N = 19 from [2] to N = 32 and decreases the production function slope from -1.68 to -2.093. We estimate the current crater production function at 6.29×10^{-7} craters km^{-2} a^{-1} for craters D >10 m. This value is intermediate from estimates by [6] and [7]. Since this new cratering rate is corrected for atmospheric loss, we assume the slope of the production function can be extended to larger D craters with some confidence up to D = 1 km. The new CPF can be represented as a power-law:

$$N = 0.0008D^{-2.093}, R^2 = 0.83 \quad (2)$$

where N represents the crater density in craters km^{-2} over 6.9 years and D is in meters. This can be written in the more traditional form in terms of log(N) and log(D):

$$\log(N) = -2.093\log(D) - 3.09691 \quad (3)$$

common for log-incremental diagrams. E_{ret} estimates are calculated for each SRC D bin utilizing both the Hartmann Production Function (HPF) [8] (that has an independent atmospheric correction) and with isochrons based on this new production function.

The Effects of Secondaries: Secondaries are those craters formed from the impact of ejecta blocks of a primary crater. A population of secondaries from a large primary can significantly increase counts of SRC, for example, near Zunil [9]. These SRC secondaries are all of one age and do not reflect a steady-state in crater production over time. Secondary cratering has been shown to follow a size-velocity, hence diameter-distance, relationship. Melosh [10] found that spall (the earliest, largest, and least shocked material ejected from a target surface) decreases in size (i.e. mass), but increases in velocity with distance away from the impactor. Graphs for four different Martian craters ranging from the D = 227 km Lyot down to the crater named Dv at D = 26 km show that the maximum secondary crater D (expressed as the fragment size) decreased with increasing distance (shown as velocity) from the primary crater according to a power-law:

$$D_{max} = v^{-\beta} \quad (4)$$

where D_{max} is the maximum fragment diameter, v is impact (and assumed launch) velocity and β is the

power-law exponent that fit the data via a least-squares method [11]. A concomitant increase in β from -2.57 to -1.46 occurred with decreasing D of the primary [11]. For Zunil, the largest rayed secondary found was D = ~230 m. The largest mapped secondaries were found to follow an approximate inverse diameter-distance relationship out to ~1750 km where the largest secondary was D = 50 m [12]. A linear fit to the maximum secondary crater D versus radial distance from Zunil (data from [12]) resulted in a strong correlation between secondary crater maximum D, D_{maxsec}, and distance, r, from the crater rim:

$$D_{maxsec} = -0.1244r + 260.35, \quad R^2 = 0.9 \qquad (5)$$

where r is in kilometers and D_{maxsec} is in meters. Solving for r, the maximum distance, r_{max}, beyond which a secondary crater of size D should not be found is:

$$r_{max} = (Dmaxsec - 260.35)/-0.1244 \qquad (6)$$

where $r_{max} \leq 0$ was ignored. We used this formula to generate buffer zones for each of our SRC D bins from 250 m down to 19 m, beyond which SRC with a larger D should theoretically not be produced from Zunil. Some of these SRC may be from other primaries, but not Zunil. These "filtered" counts were then compared to all SRC in the same distance from Zunil allowing a maximum estimate of the primary to secondary ratio for SRC in this area..

Results: SRC counts for Mars are plotted against HPF and the CPF isochrons (Figure 1). Martian isochrons generated from this new estimate evaluate E_{ret} on the order of 10 ka to 30 ka for D = 30-500 m SRC for all of Mars (mostly between ±30°). In general, CPF isochrons estimate SRC ages an order of magnitude younger than the HPF. For subregions of Mars (not shown), Amazonis-Elysium retains ejecta for ~100ka, Arabia for ~20 up to 80 ka, and Tharsis from ~10-30 ka. Ratios of All Zunil to non-Zunil SRC ranged up to 76:1 for D < 100 m (Figure 2). This has an immediate effect on E_{ret} by lowering the ages by orders of magnitude for SRC D < 200 m in this area on CPF (Figure 3). Based on our E_{ret} values, a major increase in erosion and/or deposition processes may have occurred across Mars no later than ~100 ka, removing most subsequent traces of SRC ejecta.

References: [1] Calef F. J. III et al. (2011) *LPSC XLII*, this conference. [2] Malin M.C. et al. (2006) *Science, 314*, 5805. [3] Kreslavsky M. (2007) *7th Int. Conf. Mars*, abstract #3325. [4] Tholen D.J. (1989) *Asteroids II*, 1139–1150. [5] Chappelow J. & Sharpton V. (2005) *Icarus,* 178, 40–55. [6] Daubar I.J. et al. (2010) *LPSC XLI*, abstract #1978. [7] Kennedy M.R. & Malin M.C. (2009) *AGU*, abstract #P43D-1455. [8] Hartmann W.K. (2005) *Icarus,* 174, 294–320. [9] McEwen A.S. et al. (2005) *Icarus, 176*, 3561-381. [10] Melosh H.J. (1984) *Icarus, 59*, 234-260. [11] Vickery A.M. (1987) *GRL, 14/7*, 726-729. [12] Preblich B.S. et al. (2007) *JGR, 112*, E05006.

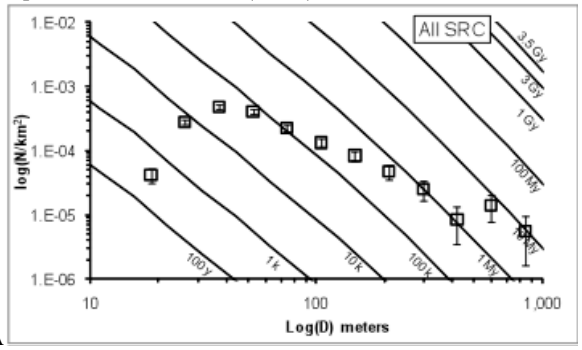

A

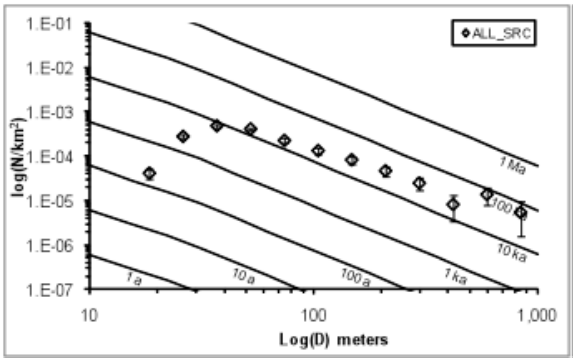

B

Figure 1: SRC E_{ret} on HPF (A) and CPF isochrons (B). Error bars are expressed as √N/A.

D (m)	All Zunil SRC	Non-Zunil SRC	Ratio
15.6-22.1	6	0	6?
22.1-31.2	26	1	26
31.2-44.2	76	0	76?
44.2-62.5	74	4	18.5
62.5-88.3	39	6	6.5
88.3-125	18	5	3.6

Figure 2: SRC secondary ratios near Zunil.

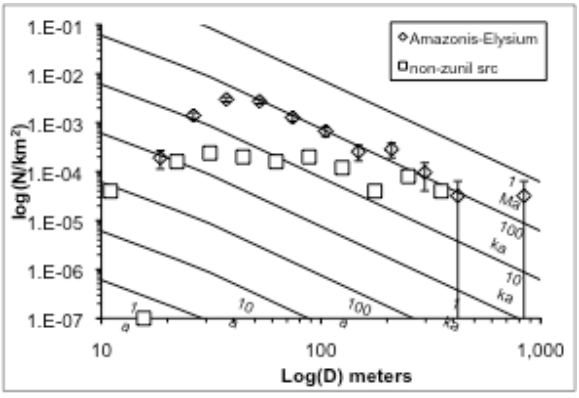

Figure 3: E_{ret} adjusted for SRC around Zunil using CPF isochrons. Error bars are expressed as √N/A.